Received: 13 February 2024 | Revised: 19 July 2024 | Accepted: 6 August 2024

DOI: 10.1002/jemt.24679

RESEARCH ARTICLE

MICROSCOPY RESEARCH & TECHNIQUE WILEY

DIY adapting SEM for low-voltage TEM imaging

Zecca Piero Antonio | Protasoni Marina | Reguzzoni Marcella | Raspanti Mario

DIMIT, Department of Medicine and Technological Innovation, University of Insubria, Varese, Italy

Correspondence
Zecca Piero Antonio, DIMIT, Department of Medicine and Technological Innovation, University of Insubria, Varese, Italy.
Email: pieroantonio.zecca@uninsubria.it

Review Editor: Alberto Diaspro

Abstract

Electron microscopy is essential for examining materials and biological samples at microscopic levels, providing detailed insights. Achieving high-quality imaging is often challenged by the potential damage high-energy beams can cause to sensitive samples. This study compares scanning electron microscopy (SEM) and transmission electron microscopy (TEM) to evaluate image quality, noise levels, and the ability to preserve delicate specimens. We used a modified SEM system with a transmitted electrons conversion accessory, allowing it to operate like a TEM but at lower voltages, thereby reducing sample damage. Our analysis included quantitative assessments of noise levels and texture characteristics such as entropy, contrast, dissimilarity, homogeneity, energy, and correlation. This comprehensive evaluation directly compared traditional TEM and the adapted SEM system across various images. The results showed that TEM provided images with higher clarity and significantly lower noise levels, reinforcing its status as the preferred method for detailed studies. However, the modified SEM system also produced high-quality images at very low acceleration voltages, which is crucial for imaging samples sensitive to high-energy exposure. The texture metrics analysis highlighted the strengths and limitations of each method, with TEM images exhibiting lower entropy and higher homogeneity, indicating smoother and more uniform textures. This study emphasizes the importance of selecting the appropriate electron microscopy method based on research needs, such as sample sensitivity and required detail level. With its conversion accessory, the modified SEM system is a versatile and valuable tool, offering a practical alternative to TEM for various applications. This research enhances our understanding of the capabilities and limitations of SEM and TEM. It paves the way for further innovations in electron microscopy techniques, improving their applicability for studying sensitive materials.

Research Highlights

- Our study introduces a modified SEM adapter enabling TEM-like imaging at reduced voltages, effectively minimizing sample damage without compromising image resolution.

- Through comparative analysis, we found that images from the modified SEM closely match the quality of traditional TEM, showcasing significantly lower noise levels.
- This advancement underscores the SEM's enhanced capability for detailed structural analysis of sensitive materials, broadening its utility across materials science and biology.

KEYWORDS
electron microscopy, image quality, low-voltage imaging, noise analysis, sample sensitivity, SEM vs. TEM

1 | INTRODUCTION

In the evolving landscape of electron microscopy, the quest for high-resolution imaging of biological and material samples under native or near-native conditions has driven significant technological advancements. Traditional transmission electron microscopy (TEM) has been the cornerstone for ultrastructural analysis, offering unparalleled resolution and depth of information. However, the high voltages typically employed in TEM can lead to sample damage, particularly for sensitive biological specimens, limiting its applicability for specific studies. In contrast, scanning electron microscopy (SEM) operates at lower voltages, reducing the risk of sample damage but traditionally offering a lower resolution than TEM.

Most manufacturers of scanning electron microscopes offer dedicated STEM adapters, essentially consisting of a detector located under the specimen, making it possible to operate a SEM like a TEM. These, however, come at a cost, require some modifications of the instrument and may not be applicable to some simpler, older microscopes.

The development of an alternative adapter that enables SEM to function similarly to TEM with no other modification, as initially explored by Eisaku Oho et al. (1987), represented a significant advancement in this field. By converting transmitted electrons into secondary electrons detectable by SEM's secondary electron detector, this adapter allows for TEM-like imaging at lower voltages, thus minimizing sample damage while providing high-resolution images. Our study builds upon this foundation, utilizing a modified version of this adapter tailored for our field emission gun SEM (FEG-SEM) to explore its potential for high-resolution imaging at reduced voltages.

Our investigation focuses on the comparative analysis of image quality, particularly examining the noise levels between images obtained from a traditional TEM and those acquired using our modified SEM equipped with the modified transmission electron adapter.

2 | MATERIALS AND METHODS

Our study used an adapter to convert a SEM into a TEM for imaging at lower voltages (https://github.com/pieroantonio/SEM-TEM). It is well known that SEM and TEM normally do not operate at the same voltages, with SEM typically working at lower voltages than TEM. This adapter is conceptually similar to the device described in the pioneering work by Eisaku Oho et al. (1987). Their device facilitated the observation of transmitted electron images in SEM by converting transmitted electrons into secondary electrons, which are then detectable by the SEM's secondary electron detector. The original design of Eisaku Oho et al. was very tall; because of physical constraints due to our specific SEM model (FEI XL-30), which could not accommodate it, we decided to reduce the height of the adapter from 40 to 10 mm (Figure 1), although this may reduce image quality. To some extent, the yield of secondary electrons is proportional to the cosine of the

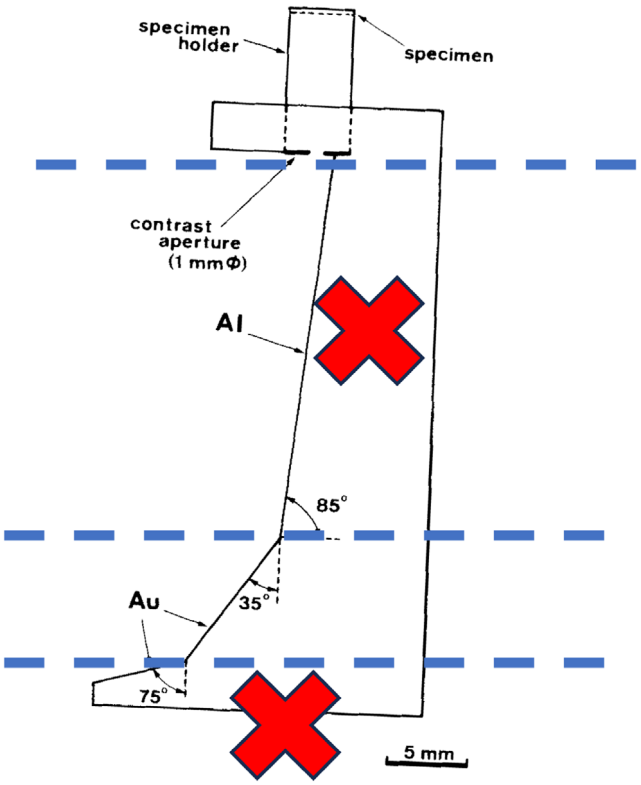

FIGURE 1 Adapter changes made. Image adapted from Eisaku et al. The dashed lines indicate the modifications we implemented to reduce the height of the adapter, ensuring it does not interfere with the backscattered electron sensor.

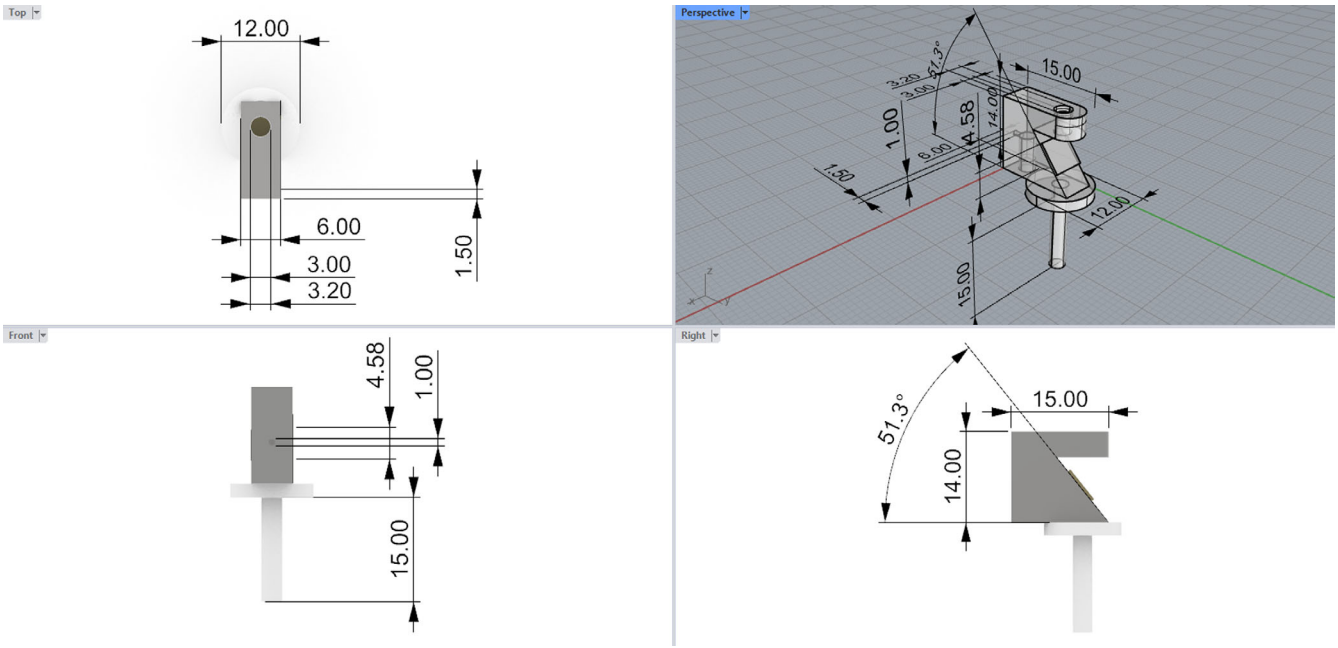

FIGURE 2 The 3D sketch illustrates the modifications made to the adapter to reduce its height from 40 to 10 mm, ensuring compatibility with the scanning electron microscopy model (FEI XL-30) without interfering with the backscattered electron sensor.

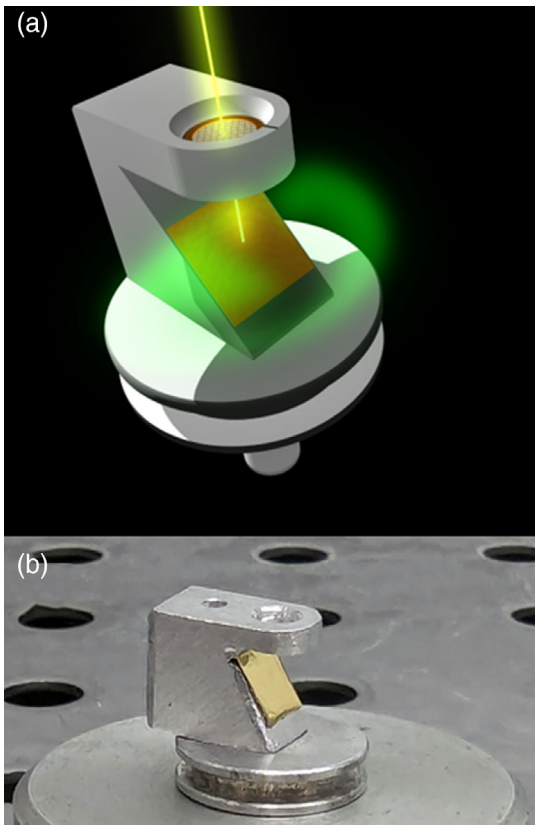

FIGURE 3 (a) The green line represents the electron beam passing through the sample on the TEM grid. After the electron beam traverses the sample, it hits the gold surface, emitting secondary electrons. These secondary electrons are then captured by the Everhart–Thornley detector. (b) Actual implementation of the adapter. In the top image, a rendering; in the bottom image, a real photo.

incidence angle of the electron beam, so increasing this angle from the 15° of the original design to the 40° of our adapter may cause some decrease in the image quality.

The adapter features a compact design, reduced in height from 40 to 10 mm, to fit within the spatial constraints of the SEM without interfering with the backscattered electron detector. The choice to incline the metal plate at approximately 50° was informed by the findings in the work by Eisaku Oho et al. (1987). Their experimental results indicated that an inclination near 85° maximizes the SE yield; however, given the physical constraints and the requirement to avoid interfering with other components of the SEM, an angle of 50° was selected. This angle balances the need for a high SE yield with the practical considerations of fitting the adapter within the SEM chamber. The specific dimensions and features of the adapter are illustrated in the accompanying design sketch. The top view shows an overall diameter of 25.00 mm, with the central support section measuring 6.00 mm in width. The sample holder section is 6.00 mm wide and 1.50 mm thick, with a 3.00 mm hole counterbored at 3.20 mm to better accommodate standard TEM grids. The front view details the total height of the adapter at 15.00 mm, with the central support section being 4.58 mm tall and the sample holder section 1.00 mm thick, positioned 15.00 mm from the base. The right view highlights the length of the inclined metal surface at 14.00 mm, set at an angle of 50°, and the sample holder extension length of 15.00 mm.

The perspective view provides an overall sense of the dimensions and relative positioning of the different sections, illustrating the compact and integrated design. This adjustment was crucial to accommodate the physical dimensions and electron optical path of our SEM, ensuring effective integration without impeding the microscope's functionality (Figures 2 and 3).

The device is straightforward in construction. It consists of a metal surface inclined at the bottom and a small holder at the top for placing ultrathin samples. The metal surface is polished, and 99.99% gold foil is applied to boost electron interactions. A key component of this device is a small hole located under the sample, which lets the electrons pass through. In practice, the electron beam from the SEM is aimed at the thin sample in the holder. Because these samples are very thin, most electrons go through them; the slight diffusion they may undergo while traversing the sample has no effect. The electrons then hit the angled metal plate, causing secondary electrons to be emitted into the chamber. This SEM conversion device offers a practical and economical way to obtain TEM-like images from a SEM without needing a full TEM setup. The SEM conversion device offers several specific advantages compared to a full TEM setup:

1. Cost-effectiveness: SEMs are generally less expensive than TEMs, and adding a simple adapter can extend existing SEM equipment's functionality without significant additional investment.
2. Ease of use: The adapter allows researchers to leverage the existing SEM infrastructure and expertise, making the transition to TEM-like imaging straightforward and accessible.
3. Reduced sample damage: Operating at lower voltages minimizes the risk of damage to sensitive samples, a significant concern in high-resolution imaging.
4. Space and maintenance: SEMs typically require less space and maintenance than TEMs, making them more suitable for smaller laboratories or facilities with limited resources.

The images obtained using this adapter were compared with those obtained from a traditional TEM. This study was carried out on human quadricep muscle samples, generously provided by Prof. Ugo Pazzaglia, adhering to the ethical guidelines set by the committee on April 7, 2011 at the Spedali Civili di Brescia and the procedures followed adhered to the World Medical Organization Declaration of Helsinki. Upon collection, the muscle tissue samples were immediately fixed by immersion in 2% glutaraldehyde and 2.5% paraformaldehyde in 0.1 M Na-cacodylate buffer solution at a pH of 7.2 at 4°C for 6 h. The samples were washed in the same buffer and postfixed for 2 h in 1% osmium tetroxide in cacodylate buffer at pH 7.2. After postfixation, the samples were dehydrated in graded ethanol (70%, 80%, 95%, and 100% every 10 min). Propylene oxide was used for two steps, each 10 min, prior to embedding in Epon 812. The samples were then sectioned into ultrathin (70 nm) slices using an RMC RTx ultramicrotome fitted with a Diatome diamond knife. The ultrathin sections were collected on honeycomb finder grids with indexed holes, stained using lead citrate 1% (10 min) and uranyl acetate saturated solution (20 min) and examined under a Jeol 1010 TEM (Raspanti et al., 2019) fitted with an Olympus MORADA digital camera at 80 kV. The fields of view in the same grids were reexamined under an FEI XL-30 FEG-SEM fitted with our custom adapter and operated at 3–5 kV (Figures 4 and 5).

Ensuring the reproducibility and reliability of the image analysis process was critical. We used six images of the same TEM grid, considering these as replicates under the same condition.

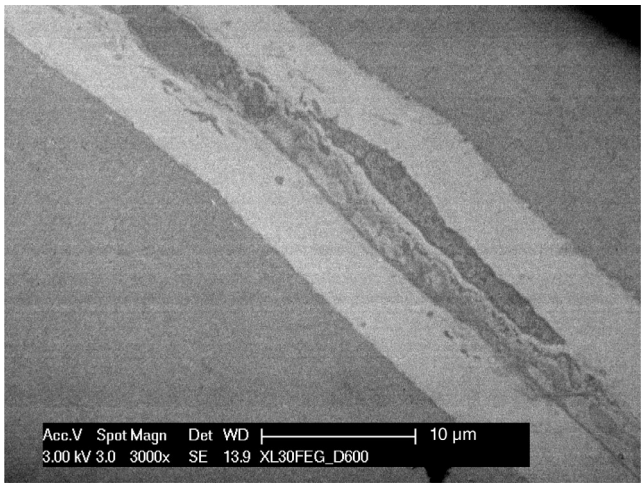

FIGURE 4 In the image's upper right and lower left corners, muscle fibers can be identified, within whose sarcoplasm the contractile elements align to form myofibrils composed of myofilaments arranged in the register. In the center of the image, the pericellular space is visible, where loose connective tissue (endomysium) with sparse collagen fibers organizes. A capillary can be seen within this connective tissue, distinguished by its endothelial lining. Adjacent to the capillary, a cellular structure is present, clearly showing the elongated nucleus of a fibroblast.

The images obtained were imported into Fiji (Schindelin et al., 2012) and cropped to remove extraneous elements such as scale bars and captions. The cropped images were then transformed into virtual stacks. These stacks were aligned using a scale-invariant feature transform (SIFT) algorithm, ensuring the images were correctly oriented and positioned relative to each other (Lowe, 2004) (Figure 6). After alignment, the image stacks were exported from Fiji into the ICY software (de Chaumont et al., 2012) and analyzed with the Gaussian Noise Estimator plugin (van der Walt et al., 2014), specifically designed to analyze images and estimate their Gaussian noise level. Gaussian noise is a common random noise affecting digital images, characterized by its normal distribution in the intensity of pixels across the image. It is characterized by its normal distribution (bell curve) in the intensity of pixels across the image. This noise can be introduced during the image capture due to various factors, including sensor temperature, electronic interference, and low lighting conditions. The primary function of the Gaussian noise estimator plugin is to quantify the amount of this noise, providing users with a numerical value that represents the standard deviation of the noise distribution. This information is crucial for researchers and analysts who need to assess the quality of their images, especially when working with delicate samples or attempting to enhance image quality through post-processing techniques. Finally, the values and data obtained were compiled and organized into Microsoft Excel.

Our study then employed Python's *scikit-image* library to conduct a texture analysis of grayscale images (van der Walt et al., 2014). This analysis was pivotal for quantifying the variability and patterns within the images. We initiated the process by loading the images directly into the Python script. We used the *greycomatrix* function from *scikit-*

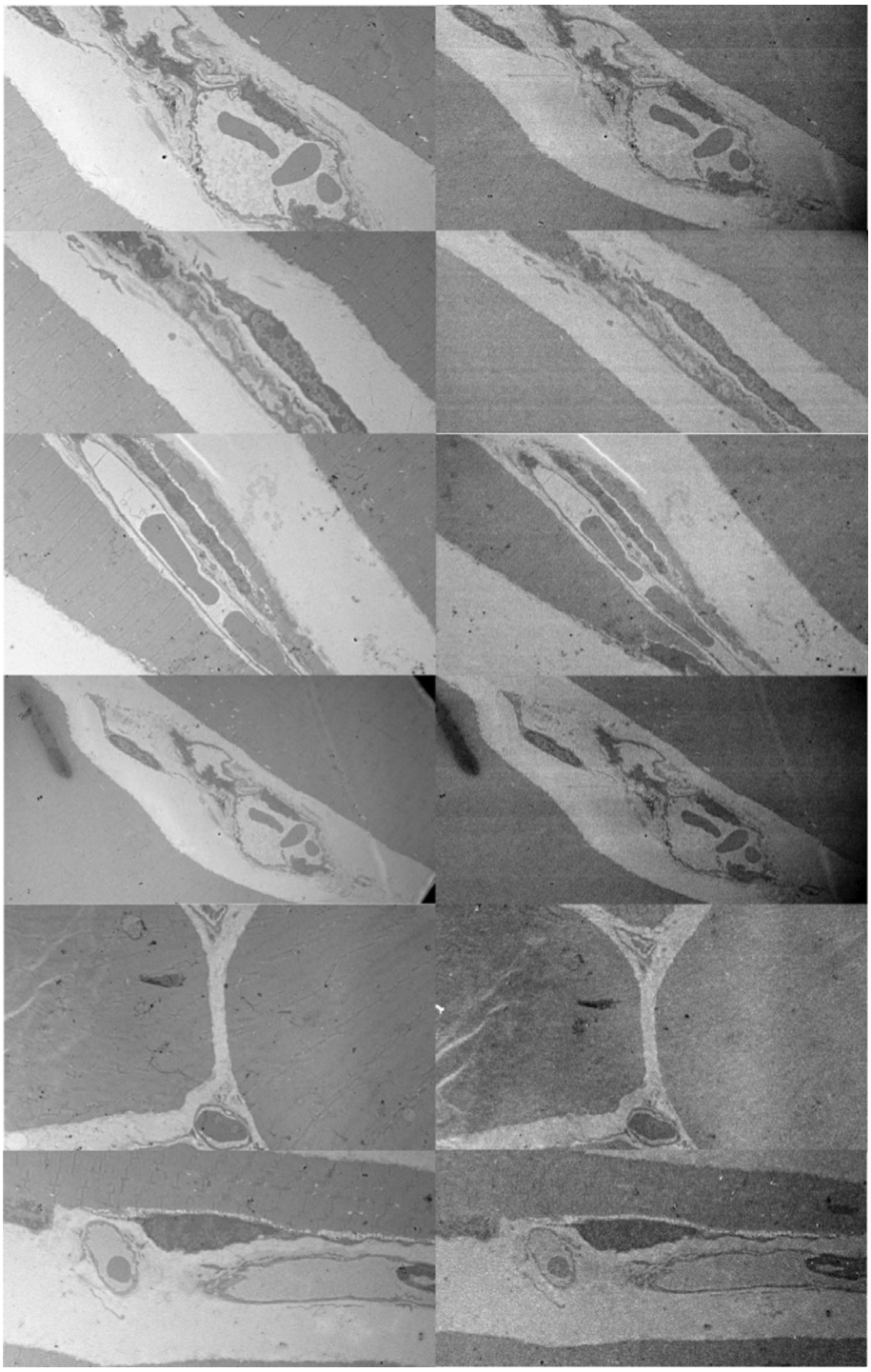

FIGURE 5 The pairs of images acquired, the left transmission electron microscopy (TEM) and the right scanning electron microscopy (SEM). Efforts were made to capture the same images at the same magnification to facilitate easy comparison. The left column displays images obtained using TEM, while the right column shows corresponding images taken with the modified SEM.

image's feature module to compute each image's gray level co-occurrence matrix (GLCM). This matrix was calculated considering pixel pairs at one pixel apart and at four different angles (0, π/4, π/2, and 3π/4 radians) to capture the texture information comprehensively across various orientations. From the GLCM, we extracted several key texture metrics, including contrast, dissimilarity, homogeneity, energy, and correlation. These metrics were averaged across all four angles to provide a unified measure of each image's texture characteristic. The contrast metric highlighted the intensity variations between pixels, while dissimilarity measured the texture's roughness. Homogeneity offered insights into the uniformity of the texture, energy quantified the texture's repetitiveness, and correlation assessed the linear dependency among the grayscale values in the image.

The image analysis workflow considered and addressed several potential sources of bias and variability. First, variability in sample preparation can introduce inconsistencies. To mitigate this, all samples were prepared using the same protocol and handled by the same operator (M.R.) to ensure uniformity.

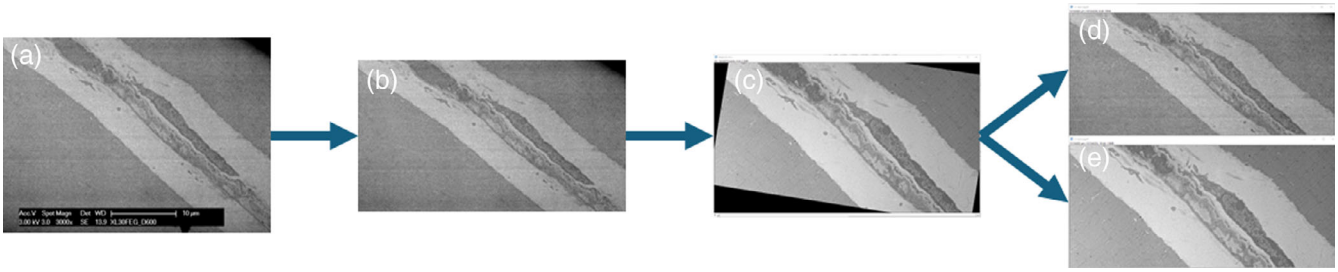

FIGURE 6 Image processing process in Fiji: Importing, cropping, registering, and recrop. (a) The original image. (b) The image was cropped to remove any elements interfering with registration, creating a virtual stack. (c) The images are rigidly registered to ensure correct orientation and positioning. Finally, the individual cropped frames are exported, resulting in corresponding scanning electron microscopy and transmission electron microscopy images for comparison. (d) SEM images registered and cropped to remove any black spaces. (e) TEM images are similarly registered and cropped.

Second, differences in imaging conditions, such as beam settings and detector sensitivity, can affect image quality. We standardized the imaging parameters for both SEM and TEM to maintain consistent conditions for all samples.

Misalignment during image registration was another potential source of error. To address this, we employed the SIFT algorithm to accurately align the images accurately, ensuring they were correctly oriented and positioned.

Human error in manual steps of the workflow can introduce bias. To minimize this, we automated as many steps as possible using software tools like Fiji and ICY, thereby reducing the potential for human error. To ensure a consistent basis for assessing noise levels across different imaging techniques, we sampled 10 white areas where only the resin was present. The rationale behind this approach was that these areas, devoid of cellular structures and other artifacts, would provide a uniform background to measure the inherent sensor noise. By focusing on regions with only resin, we minimized the influence of sample variability and structural complexity, allowing for a more precise comparison of noise levels between SEM and TEM images. Each sampled area was at least 50 × 50 pixels and positioned consistently across all images, ensuring the noise assessment was based on comparable regions.

This method ensured that our noise measurements were not confounded by variations in the biological samples themselves, providing a reliable metric for comparing the performance of the SEM and TEM imaging systems under similar conditions. By isolating the analysis to these resin-only areas, we could better understand the intrinsic noise characteristics of each imaging technique, leading to more accurate and meaningful comparisons.

Our study utilized a SEM-to-TEM conversion adapter, conceptually similar to the device described by Eisaku Oho et al. (1987), to facilitate low-voltage imaging with a modified SEM system. We acknowledge that our methods, focusing on simpler image quality and noise analysis metrics, contrast with more sophisticated approaches in recent literature. These advanced methods often involve complex algorithms and comprehensive comparative analyses to validate SEM and TEM image quality metrics, including mean structural similarity index (MSSIM), peak signal-to-noise ratio (PSNR), and various texture and morphological assessments (Brostrom & Molhave, 2022; Haoran Wang et al., 2022; Matthew et al., 2016).

TABLE 1 Table with Gaussian noise estimator values, bottom mean, and standard deviation.

	Gaussian noise estimate	
Image number	SEM	TEM
1	21.64	6.63
2	11.68	10.8
3	21.82	4.56
4	22.84	5.82
5	23.35	6.56
6	23.24	5.1
Mean	20.76 ± 4.51	6.58 ± 2.22

Note: The mean noise level for SEM images was 20.76 ± 4.51, while for TEM images, it was 6.58 ± 2.22. These results demonstrate that TEM images generally have lower noise levels than SEM images.
Abbreviations: SEM, scanning electron microscopy; TEM, transmission electron microscopy.

However, due to the lack of an objective standard for image quality evaluation in SEM and TEM, current practices largely rely on operator expertise (Haoran Wang et al., 2022). Our choice of simpler analysis methods stems from our study's practical constraints and goals. Specifically, our SEM adapter, designed as a low-cost alternative to full TEM setups, is intended to provide TEM-like imaging capabilities using existing SEM infrastructure. Given this context, our analysis focused on basic image quality metrics that are more accessible and relevant to the expected performance of our adapted SEM system. Using these simpler analyses, we aimed to demonstrate that our low-cost adapter could effectively transform a SEM into a functional TEM for specific applications, even though the image quality may not match that of a dedicated TEM. This practical approach allows for broader accessibility and utility in various research settings, particularly those with limited resources (Brostrom & Molhave, 2022; Haoran Wang et al., 2022; Matthew et al., 2016).

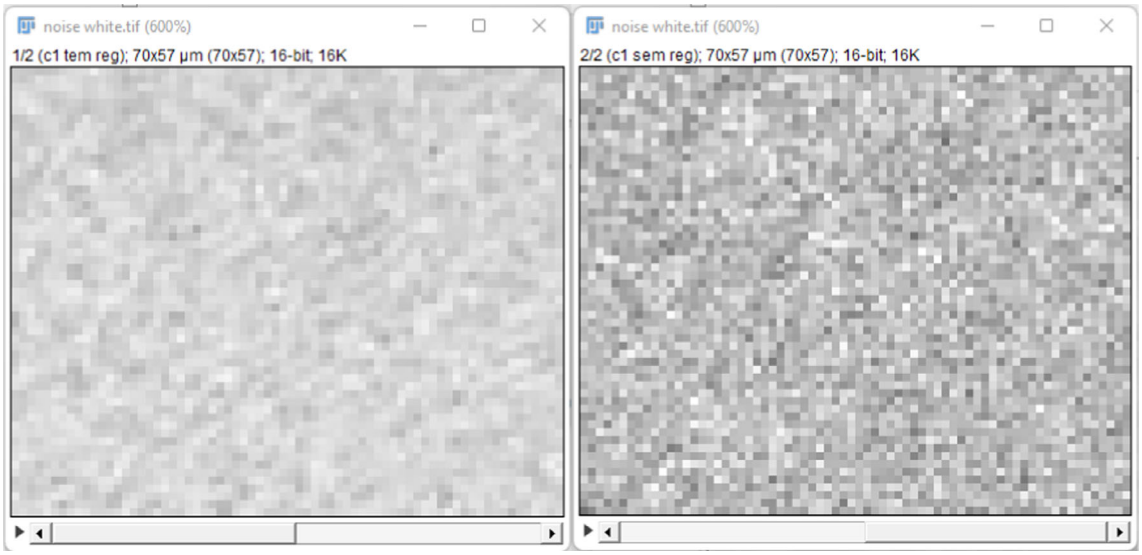

FIGURE 7 Example of a noise image in white areas. White areas where only the resin is present were sampled to evaluate sensor noise. Each sampled area had a minimum size of 50 × 50 pixels and was taken from the same position in both scanning electron microscopy and transmission electron microscopy images to ensure consistency in the noise level assessment.

TABLE 2 Texture analysis metrics extracted from the gray level co-occurrence matrix (GLCM) for TEM and SEM images.

Metric	TEM value	SEM value
Entropy	4.14	4.48
Contrast	163.44	1052.38
Dissimilarity	9.99	25.83
Homogeneity	0.097	0.037
Energy	0.030	0.017
Correlation	0.318	0.055

Note: Lower entropy and dissimilarity values and higher homogeneity and correlation values indicate that TEM images have smoother and more uniform textures.
Abbreviations: SEM, scanning electron microscopy; TEM, transmission electron microscopy.

3 | RESULTS

Our study looked at the same areas across different images to see how the noise levels compared. We focused on measuring the noise, assuming it was evenly spread as white additive Gaussian noise.

From this table, it is clear that TEM images generally have lower noise levels than SEM images. This suggests that TEM might give us clearer images with less background noise (Table 1).

The mean noise level for SEM images was 20.76 ± 4.51, while for TEM images, it was 6.58 ± 2.22. These results demonstrate that TEM images generally have lower noise levels than SEM images.

In our study, we utilized the Python library *SciPy* to perform an analysis of variance (ANOVA), enabling us to calculate the variance among different groups of images processed under varying conditions. We found a significant difference in noise levels between SEM and TEM images. The analysis yielded a significant *F*-value of 47.825 and a *p*-value of <.001, alongside a coefficient of variation of 57%, underscoring the statistical significance of the observed differences (Pauli Virtanen et al., 2020).

We also employed the *NumPy* library, a package for scientific computing in Python, to analyze key statistical metrics, including the mean, standard deviation, and coefficient of variation of the image quality metrics derived from our microscopy images. The coefficient of variation, calculated as the standard deviation divided by the mean and multiplied by 100, was used to provide a normalized measure of dispersion relative to the mean. The coefficient of variation was 57.044%, showing quite a bit of variability in the noise levels we observed (Harris et al., 2020).

To evaluate the sensor noise, we sampled 10 white areas where only the resin was present, ensuring a consistent basis for assessing the noise levels across the imaging techniques. Each sampled area was required to have a minimum size of 50 pixels by 50 pixels and was in the identical position for both imaging methods. This approach allowed us to maintain consistency in our comparison (Figure 7).

After sampling these areas, we calculated the average of the results obtained for entropy, contrast, dissimilarity, homogeneity, energy, and correlation (van der Walt et al., 2014) (Table 2).

Entropy is a measure of randomness or complexity within an image. Lower entropy values indicate that the image has more predictable and uniform textures, while higher entropy values suggest a more complex and less predictable texture. Contrast measures the difference in intensity between neighboring pixels. High contrast values indicate significant differences in intensity, resulting in a more pronounced texture, whereas low contrast values suggest a more uniform appearance with less variation in intensity. Dissimilarity reflects the variation in gray levels among pixels. Higher dissimilarity values indicate greater differences between neighboring pixel intensities, suggesting a rougher texture. Lower dissimilarity values suggest more

similarity between adjacent pixels, indicating a smoother texture. Homogeneity assesses how similar or uniform the pixels are within the image. Higher homogeneity values indicate that the pixel intensities are more uniform and consistent, suggesting a smoother texture. Lower homogeneity values indicate greater variability in pixel intensities, reflecting a more complex texture. Energy quantifies the uniformity of the texture patterns within the image. Higher energy values indicate more repetitive and consistent texture patterns, while lower energy values suggest less uniformity and greater complexity in the texture. Correlation measures the degree of correlation between a pixel and its neighboring pixels over the entire image. Higher correlation values indicate a stronger linear relationship between neighboring pixels, meaning the texture is more predictable and ordered. Lower correlation values suggest a weaker relationship and a more random texture.

4 | CONCLUSION

Our study comparing SEM with TEM highlights differences in image quality between the two methods. Our results show that TEM generally provides clearer images with less noise, making it the preferred method for capturing fine details of samples. However, SEM can still produce good-quality images with a simple accessory that functions more like a TEM. These STEM images might be slightly noisier than TEM images, but they are acceptable for many applications. This accessory is handy because it allows SEM to image samples sensitive to high-energy beams without causing damage. By reducing the energy, researchers can obtain detailed images of their samples without worrying about damaging them. While TEM might be the best choice for the highest-quality images, this modified SEM setup is a valuable option, especially for delicate samples that cannot handle the high energy of traditional TEM.

The conversion accessory makes SEM a versatile tool in the lab, providing the ability to use lower energies to protect sensitive samples while obtaining clear images for various research needs. The test parameters were optimized to achieve the best signal-to-noise ratio. Our adapter, though not a new invention, is based on previously published concepts. Modern technologies may consider such an adapter obsolete. Our method is not intended to be universal but a straightforward and cost-effective solution for specific users. We tested it on human muscle samples, and while the performance has been promising, we do not yet know if these results will be maintained with other biological samples. The practical implications of our findings are for fields such as materials science, biology and nanotechnology. For instance, researchers studying delicate biological tissues or nanomaterials susceptible to damage from high-energy beams can benefit from this approach. The modified SEM system allows for high-resolution imaging without compromising the integrity of sensitive samples. This method can be particularly advantageous in labs with limited access to TEM or those equipped with older SEM models.

Future research should focus on several key areas to further validate and expand the applicability of our findings:

1. Testing with diverse sample types: conducting additional experiments with various biological and material samples will help determine if the performance observed with human muscle samples can be replicated across different specimens.
2. Optimization of adapter design: exploring design improvements to the SEM-TEM adapter could enhance its efficiency and reduce noise levels, making it a more robust alternative to traditional TEM.
3. Comparative studies with modern technologies: comparing the modified SEM system with more recent advancements in electron microscopy will provide insights into its relative advantages and limitations, helping position it within the broader context of available imaging technologies. By addressing these future directions, researchers can build on the foundation laid by this study, enhancing the versatility and applicability of SEM modifications in various scientific fields. The goal is to provide researchers with a cost-effective high-resolution imaging solution that bridges the gap between traditional SEM and TEM capabilities, ensuring broader accessibility and utility in both research and industry settings.

AUTHOR CONTRIBUTIONS

Zecca Piero Antonio: Conceptualization; software; writing – original draft. **Protasoni Marina:** Project administration; supervision. **Reguzzoni Marcella:** Methodology; formal analysis. **Raspanti Mario:** Writing – review and editing; data curation.

ACKNOWLEDGMENTS

We thank Prof. Ugo Pazzaglia for donating the samples used in this study. Open access publishing facilitated by Universita degli Studi dell'Insubria, as part of the Wiley - CRUI-CARE agreement.

DATA AVAILABILITY STATEMENT

The data that support the findings of this study are available from the corresponding author upon reasonable request.

ORCID

Zecca Piero Antonio https://orcid.org/0000-0001-9646-4958
Raspanti Mario https://orcid.org/0000-0001-6322-1845

REFERENCES

Brostrom, A., & Molhave, K. (2022). Spatial image resolution assessment by Fourier analysis (SIRAF). *Microscopy and Microanalysis*, *3*, 1–9.

de Chaumont, F., Dallongeville, S., Chenouard, N., Herve, N., Pop, S., Provoost, T., Meas-Yedid, V., Pankajakshan, P., Lecomte, T., Le Montagner, Y., Lagache, T., Dufour, A., & Olivo-Marin, J. C. (2012). Icy: An open bioimage informatics platform for extended reproducible research. *Nature Methods*, *9*(7), 690–696.

Eisaku Oho, T. S., Adachi, K., Muranaka, Y., & Kanaya, K. (1987). An inexpensive and highly efficient device for observing a transmitted electron image in SEM. *Journal of Electron Microscopytechnique*, *5*, 8.

Haoran Wang, S. L., Ding, J., Li, S., Dong, L., & Zhaolin, L. (2022). SEM image quality assessment based on intuitive morphology and deep semantic features. *IEEE Access*, *10*, 11.

Harris, C. R., Millman, K. J., van der Walt, S. J., Gommers, R., Virtanen, P., Cournapeau, D., Wieser, E., Taylor, J., Berg, S., Smith, N. J., Kern, R., Picus, M., Hoyer, S., van Kerkwijk, M. H., Brett, M., Haldane, A., Del

Rio, J. F., Wiebe, M., Peterson, P., … Oliphant, T. E. (2020). Array programming with NumPy. *Nature*, *585*(7825), 357–362.

Lowe, D. G. (2004). Distinctive image features from scale-invariant keypoints. *International Journal of Computer Vision*, *60*(2), 19.

Matthew, Y. H., Zotta, D., Bergkoetter, M. D., & Lifshin, E. (2016). An evaluation of image quality metrics for scanning electron microscopy. *Microscopy and Microanalysis*, *22*, 572–573.

Pauli Virtanen, R. G., Oliphant, T. E., Haberland, M., Reddy, T., Cournapeau, D., Burovski, E., Peterson, P., Weckesser, W., Bright, J., van der Walt, S. J., Brett, M., Joshua Wilson, K., Millman, J., Mayorov, N., Nelson, A. R. J., Jones, E., Kern, R., Eric Larson, C. J., Carey, İ. P., … Ribeiro, F. P. (2020). Paul van Mulbregt, and SciPy 1.0 contributors., SciPy 1.0: Fundamental algorithms for scientific computing in python. *Nature Methods*, *17*(3), 11.

Raspanti, M., Reguzzoni, M., Rita Basso, P., Protasoni, M., & Martini, D. (2019). Visualizing the supramolecular assembly of collagen. *Methods in Molecular Biology*, *1952*, 33–44.

Schindelin, J., Arganda-Carreras, I., Frise, E., Kaynig, V., Longair, M., Pietzsch, T., Preibisch, S., Rueden, C., Saalfeld, S., Schmid, B., Tinevez, J. Y., White, D. J., Hartenstein, V., Eliceiri, K., Tomancak, P., & Cardona, A. (2012). Fiji: An open-source platform for biological-image analysis. *Nature Methods*, *9*(7), 676–682.

van der Walt, S. J., Schonberger, J. L., Nunez-Iglesias, J., Boulogne, F., Warner, J. D., Yager, N., Gouillart, E., Yu, T., & The Scikit-Image Contributors. (2014). Scikit-image: Image processing in python. *PeerJ*, *2*, e453.

How to cite this article: Piero Antonio, Z., Marina, P., Marcella, R., & Mario, R. (2024). DIY adapting SEM for low-voltage TEM imaging. *Microscopy Research and Technique*, 1–9. https://doi.org/10.1002/jemt.24679